photonics

MDPI

Article

Real-Time Spatial-Division Multiplexing Transmission with Commercial 400 Gb/s Transponders

Yuyang Gao [1,*], Juhao Li [2], Yu Tang [3], Lei Shen [4], Xian Zhou [1], Chunxu Zhao [3], Shikui Shen [3], Lei Zhang [4], Xiongyan Tang [3] and Zhangyuan Chen [2]

[1] School of Computer and Communication Engineering, University of Science and Technology Beijing, Beijing 100083, China; zhouxian219@gmail.com
[2] State Key Laboratory of Advanced Optical Communication Systems and Networks, Peking University, Beijing 100871, China; juhao_li@pku.edu.cn (J.L.); chenzhy@pku.edu.cn (Z.C.)
[3] Research Institute, China Unicom, Beijing 100048, China; tangy186@chinaunicom.cn (Y.T.); zhaocx62@chinaunicom.cn (C.Z.); shensk@chinaunicom.cn (S.S.)
[4] State Key Laboratory of Optical Fiber and Cable Manufacture Technology, YOFC, Wuhan 430073, China; shenlei@yofc.com (L.S.); zhanglei@yofc.com (L.Z.); tangxy@chinaunicom.cn (X.T.)
* Correspondence: yuyanggao@ustb.edu.cn

Abstract: As single-mode-fiber transmission systems are reaching their capacity limits, spatial-division multiplexing (SDM) techniques have been investigated to increase the per-fiber capacity. However, the compatibility with current single-mode transponders severely hinders the near-term deployment of SDM systems. In this paper, we experimentally propose two real-time SDM transmission schemes using commercial single-mode 400 G dual-polarized 16 quadrature amplitude modulation equipment. In the first experiment, 60 km weakly coupled single-mode 7-core fiber with a pair of fan-in and fan-out devices are adopted. In the second experiment, the fiber link consists of 60 km/150 km weakly coupled few-mode fiber (FMF) and low-modal-crosstalk mode multiplexers, in which only non-degenerate LP_{01} and LP_{02} modes are utilized. In order to investigate the effect of splice on SDM fiber links, 20-roll, 3 km multicore fibers (MCFs) and FMFs are spliced and tested in the experiments. The bit error rates of all SDM experiments are all below 4.75×10^{-2} forward-error-correction threshold of the 400 G transponders. The experimental results prove that the near-term deployment of SDM systems could be accelerated by utilizing weakly coupled MCFs or non-degenerate modes of weakly coupled FMFs which are compatible with commercial single-mode transponders without any software or hardware modifications.

Keywords: spatial-division multiplexing; weakly coupled FMF; 400 G transponders

Citation: Gao, Y.; Li, J.; Tang, Y.; Shen, L.; Zhou, X.; Zhao, C.; Shen, S.; Zhang, L.; Tang, X.; Chen, Z. Real-Time Spatial-Division Multiplexing Transmission with Commercial 400 Gb/s Transponders. *Photonics* **2024**, *11*, 231. https://doi.org/10.3390/photonics11030231

Received: 19 February 2024
Revised: 29 February 2024
Accepted: 1 March 2024
Published: 2 March 2024

1. Introduction

With the rapid development of cloud computing, 5G mobile communications and virtual reality applications and services, single-mode optical fiber (SMF) transmission systems and networks are facing great challenges on overcoming the capacity crunch. Recently, spatial-division multiplexing (SDM) fibers are widely studied as a new type of transmission media which could easily duplicate the system capacity and meet the demands of the next few decades [1,2]. From the perspective of dimensionalities, SDM fibers mainly include few-mode fibers (FMFs) and multicore fibers (MCFs). According to the crosstalk among spatial channels, SDM techniques have strongly coupled and weakly coupled transmission approaches [3–6]. The strongly coupled SDM systems usually adopt coupled-core MCFs or graded-index FMFs [7,8]. When there are N ($N = 1, 2, 3\ldots$) spatial channels in the strongly coupled SDM transmission link, $2N \times 2N$ multiple input multiple output (MIMO) digital signal processing (DSP) and coherent detection are required at the receiver side to combat crosstalk among N spatial channels with dual polarizations. There has been a lot of research in this area using dozens of spatial channels. These works

successfully prove that SDM combined with wavelength-division multiplexing (WDM) techniques have great advantages in capacity expansion [9,10]. So far, most strongly coupled SDM experiments are based on offline DSP due to the huge computational load of MIMO processing. However, current 100 G to 400 G commercial single-mode coherent optical transponders only equip 2 × 2 real-time MIMO DSP hardware for polarization diversity. The incompatibility with commercial equipment greatly hinders the near-term deployment of the SDM techniques compared to other economic and technical factors.

SDM transmission using single-mode weakly coupled MCF (WC-MCF) can effectively suppress the crosstalk among spatial channels [11,12]. Since there is no need for mode-division multiplexing (MDM), single-mode WC-MCF systems have the most straightforward migration path from SMF transmission systems. In order to suppress the inter-core crosstalk, single-mode WC-MCF usually adopts a low-index trench outside each fiber core and the core-to-core pitch is generally larger than 30 μm [13]. An increase in the number of cores means an increase in fiber diameter. For an MCF with large cladding diameter, the mechanical reliability, splice loss and production cost should be concerned at the same time, which places a limit on the number of spatial channels. Therefore, there is renewed interest in smaller diameter WC-MCFs. In particular, MCFs with the same 245 μm coating diameter as standard SMF, which are compatible with current cabling technology, have been widely explored recently.

Weakly coupled MDM approaches utilizing weakly coupled FMFs (WC-FMF) and highly selective mode multiplexer/demultiplexer (MUX/DEMUX) have also been studied to achieve practical application [14–16]. In circular-core WC-FMFs, all linear polarized (LP) modes can be divided into non-degenerate LP_{0m} modes and degenerate LP_{lm} ($l \geq 1$) modes. The LP_{lm} modes have two-fold spatial degenerate modes with the same propagation constant, labeled as LP_{lma} and LP_{lmb} modes. According to coupled-mode theory, the modal crosstalk between two LP modes is inversely related to the modal effective refractive index difference ($\min|\Delta n_{\text{eff}}|$), and the overall performance is determined by the $\min|\Delta n_{\text{eff}}|$ among all the modes [17]. Owing to a relatively large $\min|\Delta n_{\text{eff}}|$, different LP modes can be well separated in WC-FMF and the inter-LP mode crosstalk can be suppressed. However, for each pair of degenerate modes, their modal field will rotate randomly along the propagation and strong coupling will occur [18,19]. Therefore, 4 × 4 MIMO DSP is still required in WC-FMF transmission to handle the mode degeneracy and polarization. Despite some recent works having been moving towards real-time 4 × 4 MIMO processing, it is obvious that the unavoidable mixing between the degenerate modes cannot be compensated by current single-mode coherent transponders that are only equipped with 2 × 2 real-time MIMO DSP hardware [20,21].

In this paper, we experimentally demonstrate both single-mode WC-MCF and WC-FMF based SDM-WDM transmission systems employing commercial 400 G WDM transponders. In the WC-MCF transmission, link loss and end-to-end crosstalk of two optical lines constituted of single-roll 60 km or 20-roll 3 km 7-core fibers with fan-in/fan-out (FIFO) devices are characterized. Optical signal-to-noise ratio (OSNR) and bit error rate (BER) performance of the real-time system are also evaluated. In the transmission over WC-FMF, we show two non-degenerate LP-mode MDM-WDM transmission with 400 G WDM systems using 6-wavelength channels over the C band. In order to test the capability of the proposed WC-FMF and mode multiplexers in different applications, the transmission performances of 60 km, 20 × 3 km and 150 km FMF are all demonstrated. The impact of splice points on SDM systems are also investigated. To our knowledge, this is the first splice experiment of MCF and FMF link based on actual fiber cable deployment conditions. The experimental results proves that the near-term deployment of SDM systems could be accelerated by utilizing the proposed SDM transmission approaches.

2. Real-Time SDM Transmission over Single-Mode WC-MCFs

The cross-section of the single-mode MCF and the number of the cores are shown in Figure 1a. The MCF consists of seven single-mode, weakly coupled hexagonally arranged cores,

among which core 1 is the center core. The core and cladding diameters are 7.9 and 42 µm, respectively. The coating diameter is 245 µm which is the same as the standard SMF. In order to suppress the inter-core crosstalk, the core-to-core pitch is set to 41.5 µm. Besides, a low-index trench is employed outside each core, which could also decrease the bending loss. The measured refractive index of the MCF is shown in Figure 1b. The MCF has an average attenuation of about 0.21 dB/km and a dispersion coefficient of 20.9 ps/nm/km at 1550 nm. The photo of the fan-in (or fan-out) device is shown in Figure 1c. The cladding of seven standard SMFs is reduced to 41.5 µm by chemical etching process, which is the same as the pitch of the MCF. The seven thin-cladding fibers are gathered into the closest packed structure in a glass capillary and the end face is mechanically polished. The fiber bundle is actively aligned with the MCF through a six-dimensional adjustment stand and bonded with adhesive.

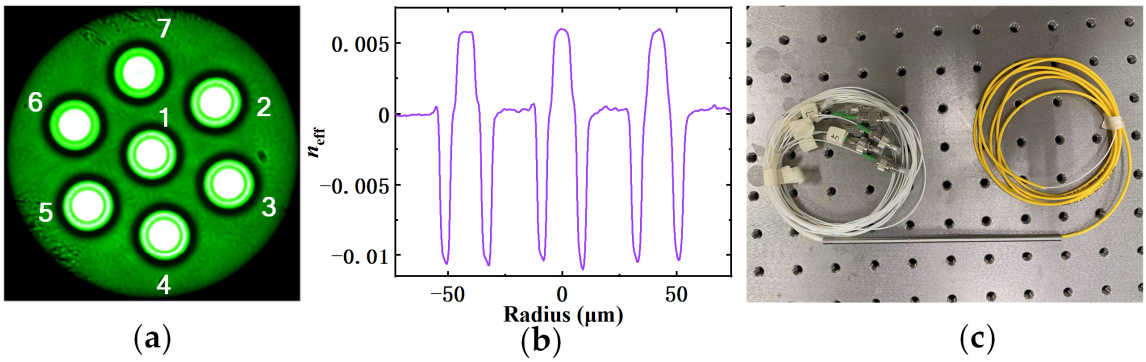

Figure 1. (**a**) Cross-section of the weakly coupled 7-core fiber. (**b**) Refractive index profile of the MCF. (**c**) Photo of a fan-in (or fan-out) device.

We construct two MCF links which are composed of single-roll 60 km MCF or 20-roll 3 km MCFs with a pair of FIFO devices. The 20-roll 3 km MCFs are spliced one by one to simulate the deployment of fiber cables in real telecommunication networks. The program of the fusion splicer (Fujikura 100 P+) is finely optimized to minimize the splice loss. The two MCF links are characterized and the results are shown in Tables 1 and 2. The diagonal elements of the matrices are link losses, while the nondiagonal elements are inter-core crosstalk. As can be seen, the link losses of core 1 (center core) in the two links are −14.0 dB and −16.2 dB, respectively. The average link losses of outer cores in the two links are −15.25 dB and −20.6 dB, respectively. For the 20-roll MCFs, the average splice losses of center core and outer cores are 0.116 dB and 0.281 dB per splice point, respectively. It can be seen that each of the six outer cores has an extra splice loss. This is because the outer core requires not only concentric alignment, but also the angular alignment. The maximum core-to-core crosstalk of the single-roll MCF and the 20-roll MCF are −48.48 dB and −48.2 dB, respectively. No obvious crosstalk degradation is observed after splicing. The low link loss and inter-core crosstalk of the 20-roll MCFs shows its great potential to be used in real telecommunication transmission systems.

The experimental setup of the real-time SDM transmission over two MCF links is illustrated in Figure 2a. The center core (core 1) and two outer cores (core 2 and 4) are chosen to test the transmission performance, since the inter-core crosstalk is minor and the outer cores have similar characteristics. The optical transceivers used in this experiment are 75 GBaud commercial 400 G dual-polarization (DP) quadrature amplitude modulation (QAM) transponders, which are installed on Digital China.2 platform. Nine transponders are divided into three sets for three cores under test. Each set consists of three transponders which are assigned the central frequencies of 191.6 THz, 193.4 THz and 196.0 THz across the C band. At the transmitter, three wavelength-selective switches (WSSs) are used as wavelength MUXes. The optical spectrum at the output of a WSS after WDM is shown in Figure 2a. Then, three single-mode erbium-doped fiber amplifiers (EDFAs) are followed to adjust the input power to balance the loss of the three cores in the MCF link. The MCF

link consists of a fan-in device, 60 km or 20 × 3 km MCFs and a fan-out device. At each output of the fan-out device, the WDM signals are demultiplexed by the other three WSSs and then detected by the corresponding 400 G receivers. The photo of the experimental setup and fibers under test is shown in Figure 2b.

Table 1. Insertion loss (diagonal data) and inter-core crosstalk (nondiagonal data) of the 60 km MCF with FIFO (Unit: dB).

Input Cores of 60 km MCF	Output Cores						
	Core 1	**Core 2**	**Core 3**	**Core 4**	**Core 5**	**Core 6**	**Core 7**
Core 1	−14.00	−50.20	<−60	−50.88	−51.40	−51.36	−51.00
Core 2	<−60	−15.70	<−60	−50.36	−52.00	<−60	−51.48
Core 3	<−60	<−60	−15.60	−51.10	<−60	−52.80	−52.70
Core 4	−51.15	−52.10	−52.34	−13.90	−51.30	−52.13	−52.40
Core 5	−50.30	−53.50	<−60	−50.68	−14.60	<−60	<−60
Core 6	−48.48	<−60	−50.40	−49.10	<−60	−16.00	<−60
Core 7	<−60	−52.33	−51.75	−50.80	<−60	<−60	−15.70

Table 2. Insertion loss (diagonal data) and inter-core crosstalk (nondiagonal data) of the 20×3 km MCF with FIFO (Unit: dB).

Input Cores of 20 × 3 km MCF	Output Cores						
	Core 1	**Core 2**	**Core 3**	**Core 4**	**Core 5**	**Core 6**	**Core 7**
Core 1	−16.20	−54.40	−52.80	−54.20	−52.50	−48.40	−53.00
Core 2	−48.20	−21.20	−50.30	−51.20	−57.70	−57.00	−57.00
Core 3	−49.40	−52.60	−20.30	<−60	<−60	−58.70	−51.70
Core 4	−49.80	−51.70	<−60	−20.10	−53.82	<−60	−58.10
Core 5	−51.00	−58.90	−58.90	−52.20	−19.30	−50.70	−58.90
Core 6	−51.10	−56.80	−56.80	−56.80	−51.70	−21.40	−55.10
Core 7	−50.70	−56.90	−51.10	−56.90	−56.90	−56.90	−21.30

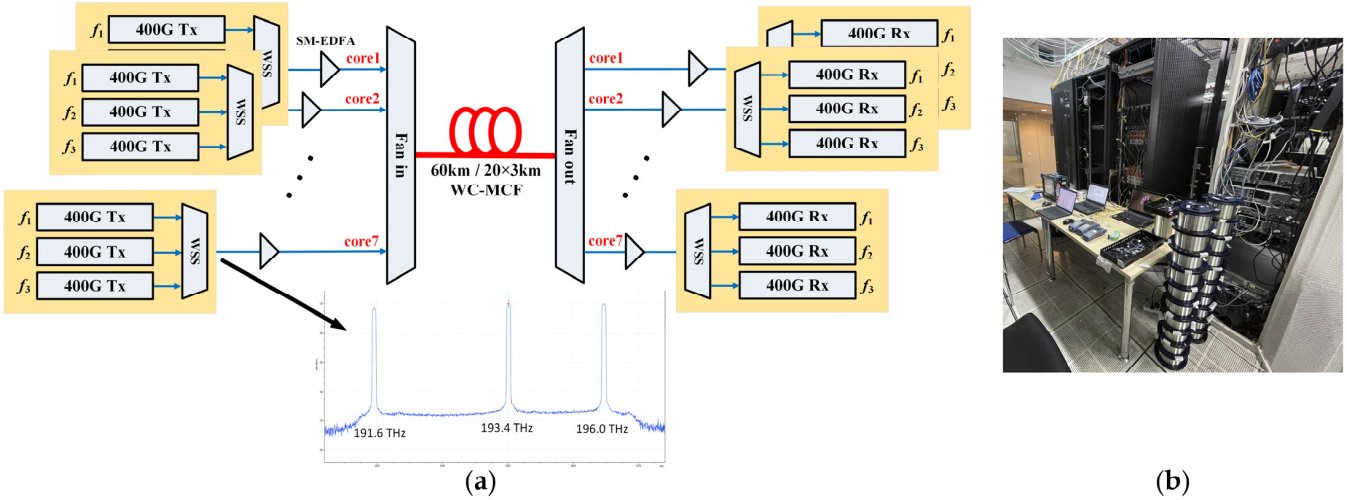

Figure 2. (**a**) Experimental setup of the real-time SDM-WDM system (optical spectrum at the output of a WSS). (**b**) Photo of the experimental setup and fibers under test.

The OSNR and BER performance versus input power of core 1, 2 and 4 at 193.4 THz in two cases are depicted in Figure 3a. The launched power varies from −20 dBm to 7 dBm by adjusting the output power of the EDFAs online. After each adjustment of launching power, the system will run for 5 min before recording data. The OSNR of each channel increases with the input power. The three channels of the single-roll scheme and center-core channel in the 20-roll scheme have similar OSNR performance, while the outer-core channels in the 20-roll system have an OSNR penalty of about 4 dB compared to other channels because of the extra insertion loss. The insertion loss comes from the 19 fusion splice points with slightly angular misalignment. Figure 3b exhibits the pre-forward-error-correction (FEC) BER performance of the six channels in the two schemes. As can be seen, BER of all channels are below the FEC threshold (4.75×10^{-2}) of the 400 G receivers. At the sensitivity limit of the receiver, the 20-roll MCF transmission system ran for 6 h, and the BER was still below the threshold of 4.75×10^{-2} during this time. It should be noted that there is no hardware or software modification on the transponders, which means that the two weakly coupled MCF systems are highly compatible with commercial single-mode transceivers.

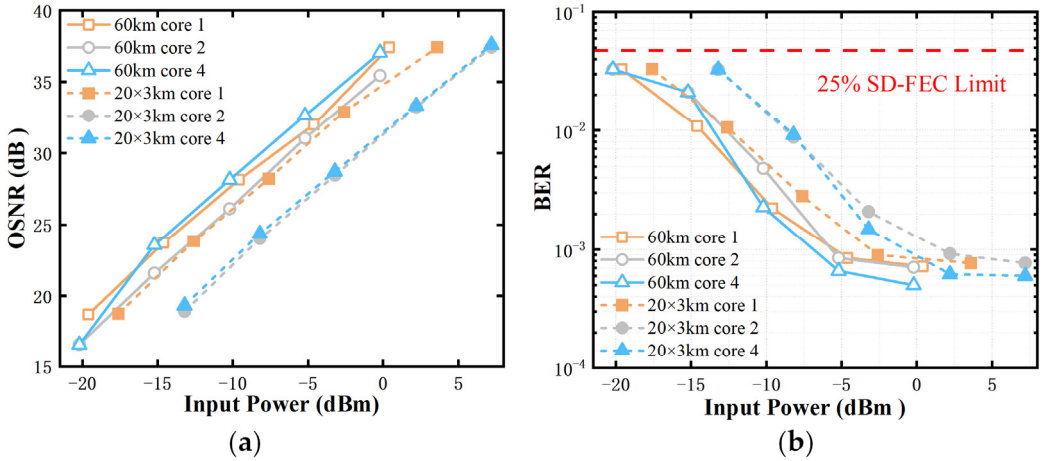

Figure 3. (**a**) OSNR and (**b**) BER curves versus input power of core 1, 2 and 4 in single-roll and 20-roll cases.

3. Real-Time MDM Transmission Using Non-Degenerate LP Modes of the WC-FMF

The modal field of non-degenerate LP modes in the WC-FMF are invariant under the rotation, so 4 × 4 MIMO DSP are not necessary. In this paper, we only employ non-degenerate LP modes in the WC-FMF link. Therefore, the whole system could be compatible with commercial single-mode transponders. Figure 4a shows the designed and fabricated refractive index profile of the proposed weakly coupled FMF and the effective refractive index of the supported LP modes. The fiber has a normalized frequency V of 4.8 and a relative refractive index difference between the fiber core and cladding (Δn) of 0.6%. The FMF support LP_{01}, LP_{11}, LP_{21} and LP_{02} modes. As is known, the n_{eff} of all LP modes of a step-index WC-FMF are between n_{eff} of the cladding (n_{cl}) and core (n_{co}). Given that the core and cladding index difference (Δ) remains constant, if the n_{eff} of all LP modes distribute equally between n_{cl} and n_{co}, the min $|\Delta n_{eff}|$ could achieve its maximum. Therefore, the design principle of WC-FMF is to adjust the n_{eff} of all LP modes to approach equal spacing as much as possible under a certain Δ. If we introduce a small perturbed refractive index ring area in the fiber core, the n_{eff} of the guided LP mode can be adjusted. Since different LP modes have different power spatial distributions, only one ring structure cannot satisfy the n_{eff} adjustment for all modes. Therefore, multiple-ring-core structure, considering the power distributions of all LP modes, can be utilized to achieve a large min $|\Delta n_{eff}|$ and the inter-LP-mode crosstalk can be effectively suppressed. In this paper, three perturbed rings areas are adopted in the core to adjust the n_{eff} of four LP modes to maximize the min $|\Delta n_{eff}|$ as much as possible. In order to reduce the bending sensitivity of high-order LP modes, a depressed-index fluorine-doped trench is applied in the cladding. The min $|\Delta n_{eff}|$ of the

fabricated FMF is 1.89 × 10^{-3} lying between LP_{21} and LP_{02} modes, which can effectively suppress the modal crosstalk between them. The attenuations of the four LP modes are all lower than 0.227 dB/km thanks to the depressed-index trench.

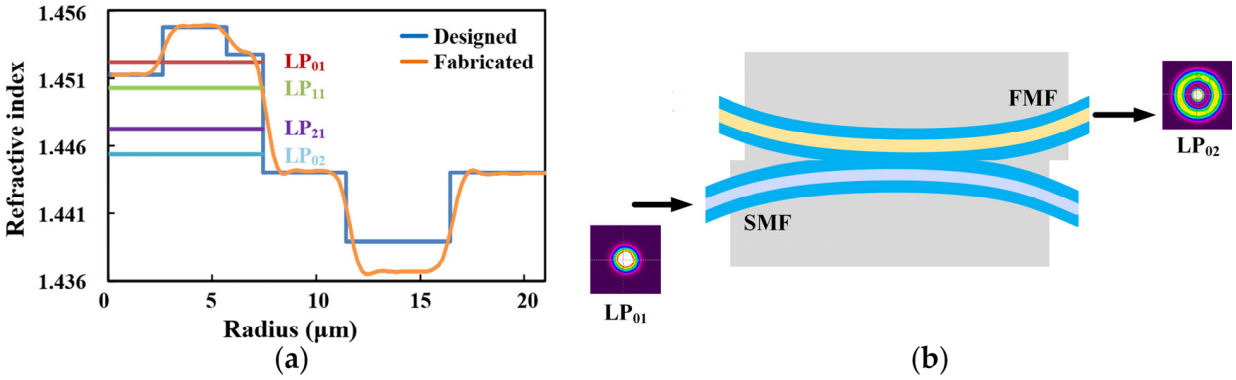

Figure 4. (**a**) Refractive index profile of the FMF and n_{eff} of the four LP modes. (**b**) Structure of the side-polished MSC.

The mode MUX/MDEMUX in this work are consisted of side-polished all-fiber mode-selective couplers (MSC), the structure of which is shown in Figure 4b. MSC is a directional fiber coupler providing exclusive mode-coupling between the fundamental mode of the SMF and a specific higher order mode of the FMF when the propagation constants of the two modes are identical. Phase mismatch will increase the insertion loss and decrease the modal selectivity. In this paper, the mode MUX is made up by cascading LP_{01} and LP_{02} MSCs whose FMF is the same as the transmission fiber. On one hand, identical fibers can reduce the insertion loss induced by mode field mismatch at the connection point between the MSC and the transmission FMF. On the other hand, since the transmission FMF has been finely designed to enlarge the $\min|\Delta n_{eff}|$, it could effectively decrease the modal crosstalk. The insertion loss for a pair of LP_{01} MSCs are about 2 dB, while it is 6 dB for a pair of LP_{02} MSCs.

Similar to the two links in MCF transmission, we also constructed single-roll 60 km and 20-roll 3 km FMF links to simulate real deployment of the fiber cable. Besides, 5-roll (60 + 25 + 25 + 25 + 15 = 150 km) FMFs are constructed to test the long-haul real-time MDM transmission performance. Each transmission link consists of an FMF and a pair of mode MUX/DEMUX for LP_{01} and LP_{02} modes. The insertion loss and modal crosstalk matrices of the three FMF links are measured. The results are shown in Tables 3–5. Compared to the single-roll 60 km FMF link, the extra insertion loss of the 20-roll FMF link is 0.3 dB and 0.47 dB for LP_{01} and LP_{02} modes, respectively. It can be seen that the insertion loss and crosstalk of the 20-roll 3 km FMF link only degrade slightly due to the 19 splice points. The modal crosstalk of the 150 km FMF link is larger than the other two cases, which could be balanced by adjusting the input power of the two modes.

Table 3. Insertion loss (diagonal data) and inter-mode crosstalk (nondiagonal data) of the 60 km FMF with mode MUX (Unit: dB).

Input Modes of the 60 km FMF	Output Modes	
	LP_{01}	**LP_{02}**
LP_{01}	−14.42	−34.21
LP_{02}	−34.12	−19.63

Table 4. Insertion loss (diagonal data) and inter-mode crosstalk (nondiagonal data) of the 20×3 km FMF with mode MUX (Unit: dB).

Input Modes of the 20 × 3 km FMF	Output Modes	
	LP_{01}	LP_{02}
LP_{01}	−14.72	−33.23
LP_{02}	−32.70	−20.10

Table 5. Insertion loss (diagonal data) and inter-mode crosstalk (nondiagonal data) of the 150 km FMF with mode MUX (Unit: dB).

Input Modes of the 150 km FMF	Output Modes	
	LP_{01}	LP_{02}
LP_{01}	−33.87	−52.89
LP_{02}	−51.00	−41.24

Figure 5 shows the experimental setup of real-time 2-LP-mode MDM-WDM transmission with commercial 400 G transponders. Twelve 400 G transponders are utilized in this experiment and each mode carries six wavelengths. The six central frequencies of the transponders for each mode are set to 191.6 THz, 191.7 THz, 193.3 THz, 193.4 THz, 196 TH and 196.1 THz which are at the beginning, middle and end of the C band. Other parameters of the transponders are the same as the MCF transmission. The two WDM signals are amplified by two EDFAs and then mode-multiplexed by the all-fiber mode MUX. After the FMF transmission, the MDM signals are demultiplexed by the mode DEMUX into two SMFs. Finally, the single-mode WDM signals are demultiplexed by another two WSSs and fed into the receivers for detection.

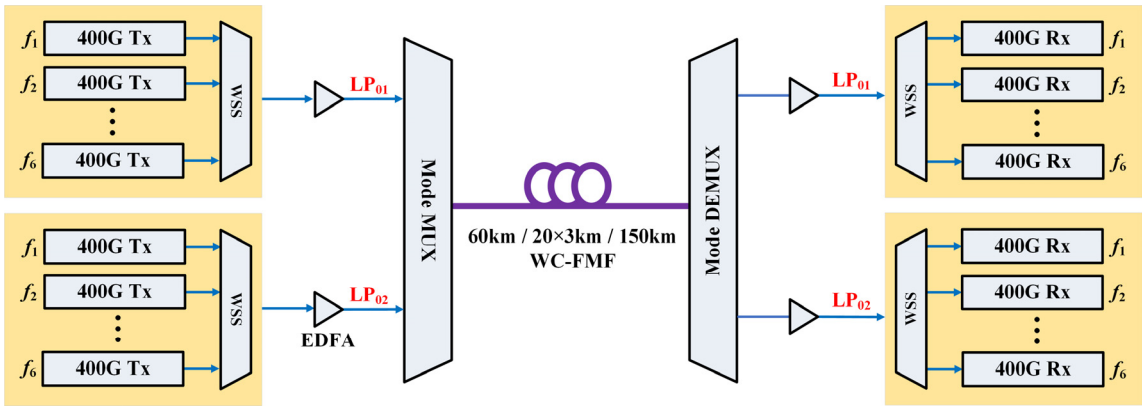

Figure 5. Experimental setup of real-time non-degenerate 2-LP-mode MDM-WDM transmission with commercial 400 G transponders.

In the experiment of a single-roll 60 km FMF link, the OSNR and BER performances versus input power of LP_{01} and LP_{02} modes in single-mode and MDM transmission are both measured. The results of the four cases (LP_{01} only, LP_{02} only, LP_{01} MDM, LP_{02} MDM) are shown in Figure 6a,b. Because the performance of different WDM channels is similar, the results at 193.4 THz is demonstrated only. The modal crosstalk is regarded as noise when calculating OSNR. It can be seen that as the input power increases, the OSNR increases while the BER decreases in each of the four cases. The performance of single-mode transmission is better than the MDM transmission due to the modal crosstalk. Figure 6c shows the BERs of the MDM transmission at six frequencies, in which the input power of LP_{01} and LP_{02} modes are 7.66 dBm and 10.07 dBm, respectively. It can be seen the BERs are all below the FEC threshold. The BER and OSNR performance of the 20-roll

FMF link are shown in Figure 6d,e, respectively. It can be seen that the BER curves of the 20-roll 3 km FMF link are flatter than the those of the single-span 60 km FMF link. This is because the extra modal crosstalk caused by the 19 splice points slow down the increase of the OSNR. At the sensitivity limit of the receiver, the 20-roll MDM transmission system ran for 6 h, and the BER was still below the threshold of 4.75×10^{-2} during this time. Figure 6f shows the BERs of the 20-roll MDM transmission at six frequencies, in which the input power of LP_{01} and LP_{02} modes are 7.85 dBm and 10.1 dBm, respectively. It can be seen the BERs are all below the FEC threshold as well. The BER and OSNR performance of the 150 km FMF link are shown in Figure 6g,h, respectively. It can be seen that in both single-mode and MDM transmission, the performance of LP_{02} mode is worse than that of LP_{01} mode. This is because no EDFA is employed within the 150 km FMF, the total loss of LP_{02} modes is larger than LP_{01} mode which leads to a small OSNR. Figure 6i shows the BERs of the 150 km MDM transmission at six frequencies, in which the input power of LP_{01} and LP_{02} modes are 16.15 dBm and 16.32 dBm, respectively. It can be seen the BERs are all below the FEC threshold in which the margin of LP_{02} mode is minor. The experiment proves that the proposed non-degenerate LP mode MDM system with all-fiber MSCs can achieve 150 km repeaterless transmission using commercial 400 G transponders.

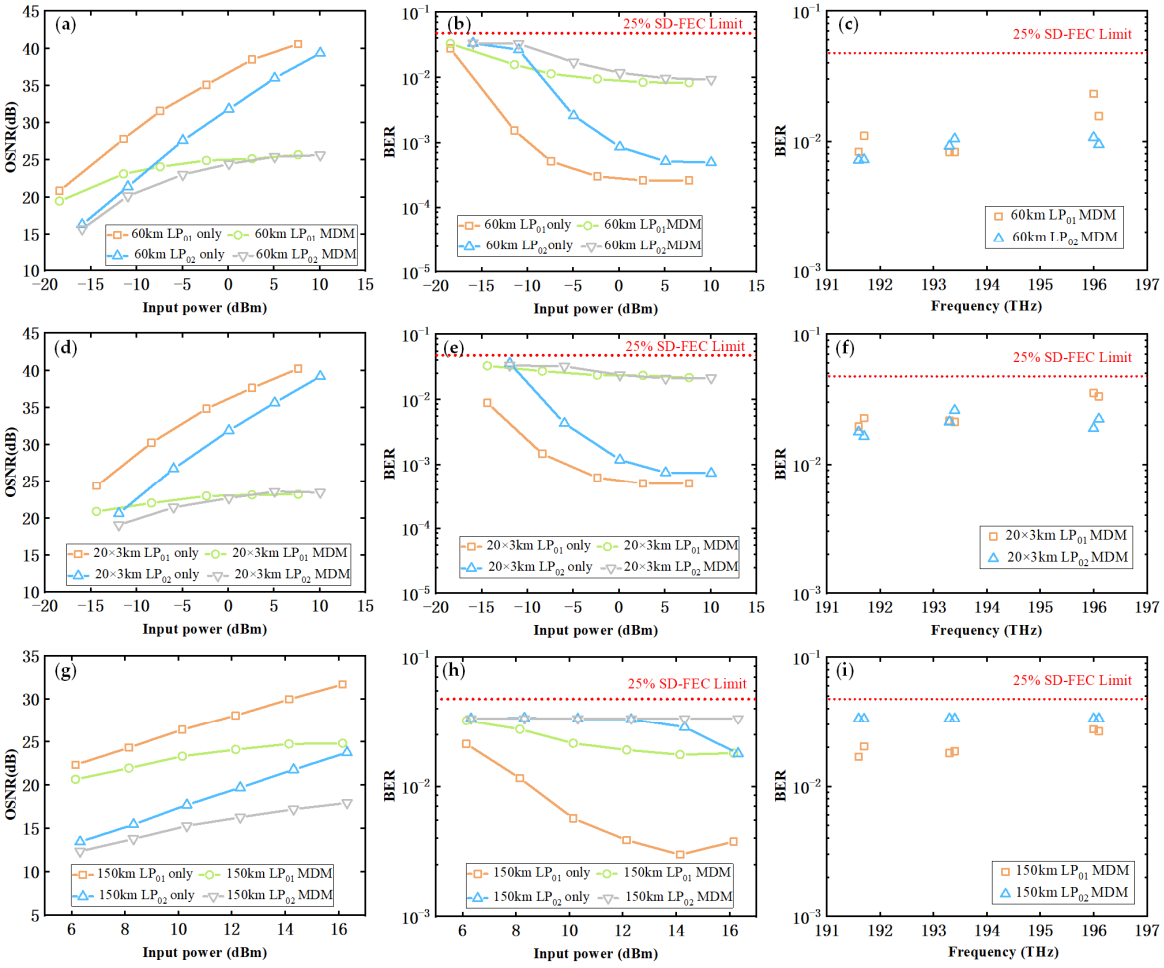

Figure 6. (**a**) OSNR curves versus input power of 60 km single-mode and MDM transmission. (**b**) BER curves versus input power of 60 km single-mode and MDM transmission. (**c**) BER over the C-band of 60 km MDM transmission. (**d**) OSNR curves versus input power of 20 × 3 km single-mode and MDM transmission. (**e**) BER curves versus input power of 20 × 3 km single-mode and MDM transmission. (**f**) BER over the C-band of 20 × 3 km MDM transmission. (**g**) OSNR curves versus input power of 150 km single-mode and MDM transmission. (**h**) BER curves versus input power of 150 km single-mode and MDM transmission. (**i**) BER over the C-band of 150 km MDM transmission.

4. Discussions and Conclusions

In this paper, we propose two real-time SDM transmission approaches which are compatible with commercial 400 G coherent single-mode transponders. In the first scheme, a 60 km single-mode WC-MCF with a pair of fan-in and fan-out devices is employed. In the second experiment, the fiber link is composed of 60 km/150 km WC-FMF and low-modal-crosstalk mode multiplexers, in which only non-degenerate LP_{01} and LP_{02} modes are adopted. In all transmission tests, the BERs are below the FEC threshold of the 400 G transponders. Therefore, SDM transmission using single-mode WC-MCF or WC-FMF with non-degenerate LP modes are two effective approaches which are compatible with current commercial single-mode coherent transponders.

In both MCF and FMF transmissions, the influence of splice points is investigated. For the MCFs, the splice points only affect insertion loss but do not introduce inter-core crosstalk. The experimental results show that the six outer cores have larger splice losses than the center core. This shows that the outer cores should also be angularly aligned rather than simply having cladding alignment. Despite the transmission capacity of the MCF being seven times that of SMF, extra insertion loss leads to a shorter transmission length. Therefore, single-mode WC-MCF is currently more suitable for medium- or short-distance large-capacity transmission. Furthermore, the reduction of the splice loss should be investigated for MCFs by employing CO_2 lasers and more precise alignment techniques. For the FMFs, the experimental results show that the splice loss is much smaller than the average level of MCF, close to the level of commercial SMF. However, weakly coupled FMF transmission over non-degenerate LP modes is suitable for medium or short distance as well. This is because the modal crosstalk—and not the loss introduced by the splice point—is the main issue. Since the length of one span of optical cable is 2~3 km, a long-distance transmission link will contain lots of splice points. The accumulated modal crosstalk will reduce the OSNR of the system. Besides, the distributed modal coupling along the FMF transmission and mode MUX/DEMUX will also inevitably introduce modal crosstalk.

Compared to elliptical core FMF transmission using commercial single-mode transceivers, the proposed two SDM transmission schemes increase the transmission distance from 1 km to dozens of kilometers [22]. Although the mode-group division multiplexing could achieve MIMO-free transmission as well, the output fibers are FMFs rather than SMFs, which are not compatible with commercial single-mode coherent transceivers [23]. in addition, employing only non-degenerate LP modes could accelerate use of the SDM technique. Further capacity upgrade of the system could be implemented using degenerate LP modes with 4×4 real-time MIMO processing when the hardware is available with a low cost.

Compared to single-mode WC-MCFs, WC-FMF with 125 μm cladding diameter has higher spatial channel density, as signals traveling in orthogonal spatial modes share the same fiber core. Since WC-FMFs have a step-index profile similar to commercial SMF, its production process is compatible with the mature plasma chemical vapor deposition technique. Its mechanical reliability and splice accuracy are similar to commercial SMF as well, which is also proved by our experiments. Additionally, although the few-mode multicore fibers can combine two dimensionalities and have a higher spatial density, the length of current single-roll FM-MCF rarely exceeds 10 km due to production yield. Therefore, the two approaches proposed in this paper are more likely to be deployed in the near-term with only one dimensionality extension.

Author Contributions: Conceptualization, Y.G., L.S. and S.S.; methodology, Y.G. and Y.T.; software, Y.G.; validation, J.L. and C.Z.; writing—original draft preparation, Y.G., L.S. and Y.T.; writing—review and editing, Y.G. and Y.T.; supervision, X.Z. and Z.C.; project administration, X.T. and L.Z.; funding acquisition, Y.G. and J.L. All authors have read and agreed to the published version of the manuscript.

Funding: This research was funded by the National Natural Science Foundation of China, grant number 62101009, U20A20160. Pengcheng Zili Project, grant number PCL2023AS2-4.

Institutional Review Board Statement: Not applicable.

Informed Consent Statement: Not applicable.

Data Availability Statement: The original contributions presented in the study are included in the article, further inquiries can be directed to the corresponding author.

Conflicts of Interest: The authors declare no conflicts of interest.

References

1. Richardson, D.J.; Fini, J.M.; Nelson, L.E. Space-division multiplexing in optical fibres. *Nat. Photonics* **2013**, *7*, 354–362. [CrossRef]
2. Li, G.; Bai, N.; Zhao, N.; Xia, C. Space-division multiplexing: The next frontier in optical communication. *Adv. Opt. Photonics* **2014**, *6*, 413–487. [CrossRef]
3. Ryf, R.; Randel, S.; Gnauck, A.H.; Bolle, C.A.; Sierra, A.; Mumtaz, S.; Esmaeelpour, M.; Burrows, E.C.; Essiambre, R.-J.; Winzer, P.J.; et al. Mode-division multiplexing over 96 km of few-mode fiber using coherent 6 × 6 MIMO processing. *J. Light. Technol.* **2012**, *30*, 521–531. [CrossRef]
4. Fontaine, N.K.; Ryf, R.; Chen, H.; Benitez, A.V.; Lopez, J.A.; Correa, R.A.; Guan, B.; Ercan, B.; Scott, R.P.; Yoo, S.B.; et al. 30×30 MIMO transmission over 15 spatial modes. In Proceedings of the Optical Fiber Communication Conference, San Diego, CA, USA, 22–26 March 2015.
5. Hu, T.; Li, J.; Zhang, Y.; Li, Z.; He, Y.; Chen, Z. Wavelength-Insensitive Weakly Coupled FMFs and Components for the MDM-GPON. *IEEE Photon. Technol. Lett.* **2018**, *30*, 1277–1280. [CrossRef]
6. Igarashi, K.; Park, K.J.; Tsuritani, T.; Morita, I.; Kim, B.Y. All-fiber-based selective mode multiplexer and demultiplexer for weakly-coupled mode-division multiplexed systems. *Opt. Commun.* **2018**, *408*, 58–62. [CrossRef]
7. Ryf, R.; Alvarado-Zacarias, J.C.; Wittek, S.; Fontaine, N.K.; Essiambre, R.J.; Chen, H.; Amezcua-Correa, R.; Sakuma, H.; Hayashi, T.; Hasegawa, T.; et al. Coupled-Core Transmission over 7-Core Fiber. In Proceedings of the Optical Fiber Communication Conference, San Diego, CA, USA, 3–7 March 2019.
8. Sillard, P.; Molin, D.; Bigot-Astruc, M.; De Jongh, K.; Achten, F.; Velázquez-Benítez, A.M.; Amezcua-Correa, R.; Okonkwo, C.M. Low-Differential-Mode-Group-Delay 9-LP-Mode Fiber. *J. Light. Technol.* **2016**, *34*, 425–430. [CrossRef]
9. Shibahara, K.; Mizuno, T.; Doowhan, L.; Miyamoto, Y.; Ono, H.; Nakajima, K.; Saitoh, S.; Takenaga, K.; Saitoh, K. DMD-Unmanaged Long-Haul SDM Transmission Over 2500-km 12-core × 3-mode MC-FMF and 6300-km 3-mode FMF Employing Intermodal Interference Cancelling Technique. In Proceedings of the Optical Fiber Communication Conference, San Diego, CA, USA, 11–15 March 2018.
10. Ryf, R.; Fontaine, N.K.; Wittek, S.; Choutagunta, K.; Mazur, M.; Chen, H.; Alvarado-Zacarias, J.C.; Amezcua-Correa, R.; Capuzzo, M.; Kopf, R.; et al. High-Spectral-Efficiency Mode-Multiplexed Transmission over Graded-Index Multimode Fiber. In Proceedings of the 2018 European Conference on Optical Communication (ECOC), Rome, Italy, 23–27 September 2018.
11. Zhu, B.; Taunay, T.; Fishteyn, M.; Liu, X.; Chandrasekhar, S.; Yan, M.F.; Fini, J.M.; Monberg, E.M.; Dimarcello, F.V. 112 Tb/s space-division multiplexed DWDM transmission with 14-b/s/Hz aggregate spectral efficiency over a 768-km seven-core fiber. *Opt. Express* **2011**, *19*, 16665–16671. [CrossRef] [PubMed]
12. Zhu, B.; Taunay, T.F.; Yan, M.F.; Fini, J.M.; Fishteyn, M.; Monberg, E.M.; Dimarcello, F.V. Seven-core multicore fiber transmissions for passive optical network. *Opt. Express* **2010**, *18*, 11117–11122. [CrossRef] [PubMed]
13. Saitoh, K.; Matsuo, S. Multicore Fiber Technology. *J. Light. Technol.* **2016**, *34*, 55–66. [CrossRef]
14. Soma, D.; Beppu, S.; Wakayama, Y.; Igarashi, K.; Tsuritani, T.; Morita, I.; Suzuki, M. 257-Tbit/s Weakly Coupled 10-Mode C + L-Band WDM Transmission. *J. Light. Technol.* **2018**, *36*, 1375–1381. [CrossRef]
15. Soma, D.; Wakayama, Y.; Igarashi, K.; Tsuritani, T. Partial MIMO-based 10-Mode-Multiplexed Transmission over 81 km Weakly-coupled Few-mode Fiber. In Proceedings of the Optical Fiber Communication Conference, Los Angeles, CA, USA, 19–23 March 2017.
16. Cui, J.; Gao, Y.; Huang, S.; Yu, J.; Liu, J.; Jia, J.; He, Y.; Chen, Z.; Li, J. Five-LP-Mode IM/DD MDM Transmission Based on Degenerate-Mode-Selective Couplers with Side-Polishing Processing. *J. Light. Technol.* **2023**, *41*, 2991–2998. [CrossRef]
17. Ge, D.; Gao, Y.; Yang, Y.; Shen, L.; Li, Z.; Chen, Z.; He, Y.; Li, J. A 6-LP-mode ultralow-modal-crosstalk double-ring-core FMF for weakly coupled MDM transmission. *Opt. Commun.* **2019**, *451*, 97–103. [CrossRef]
18. Li, J.; Du, J.; Ma, L.; Li, M.; Jiang, S.; Xu, X.; He, Z. Coupling analysis of non-circular-symmetric modes and design of orientation-insensitive few-mode fiber couplers. *Opt. Commun.* **2017**, *383*, 42–49. [CrossRef]
19. Love, J.D.; Riesen, N. Mode-selective couplers for few-mode optical fiber networks. *Opt. Lett.* **2012**, *37*, 3990–3992. [CrossRef] [PubMed]
20. Beppu, S.; Igarashi, K.; Kikuta, M.; Soma, D.; Nagai, T.; Saito, Y.; Takahashi, H.; Tsuritani, T.; Morita, I.; Suzuki, M.; et al. Weakly coupled 10-mode-division multiplexed transmission over 48-km few-mode fibers with real-time coherent MIMO receivers. *Opt. Express* **2020**, *28*, 19655–19668. [CrossRef] [PubMed]
21. Beppu, S.; Kikuta, M.; Igarashi, K.; Mukai, H.; Shigihara, M.; Saito, Y.; Soma, D.; Takahashi, H.; Yoshikane, N.; Tsuritani, T.; et al. Long-Haul Coupled 4-Core Fiber Transmission Over 7200 Km With Real-Time MIMO DSP. *J. Light. Technol.* **2022**, *40*, 1640–1649. [CrossRef]

22. Ip, E.; Milione, G.; Li, M.J.; Cvijetic, N.; Kanonakis, K.; Stone, J.; Peng, G.; Prieto, X.; Montero, C.; Moreno, V.; et al. SDM transmission of real-time 10GbE traffic using commercial SFP + transceivers over 0.5km elliptical-core few-mode fiber. *Opt. Exp.* **2015**, *23*, 17120–17126. [CrossRef] [PubMed]
23. Benyahya, K.; Simonneau, C.; Ghazisaeidi, A.; Muller, R.; Bigot, M.; Sillard, P.; Jian, P.; Labroille, G.; Renaudier, J.; Charlet, G. 200 Gb/s Transmission over 20 km of FMF Fiber using Mode Group Multiplexing and Direct Detection. In Proceedings of the 2018 European Conference on Optical Communication (ECOC), Rome, Italy, 23–27 September 2018.